Journal of Catalysis 262 (2009) 199–205

Contents lists available at ScienceDirect

Journal of Catalysis

www.elsevier.com/locate/jcat

Effect of strong metal–support interaction on the catalytic performance of Pd/TiO_2 in the liquid-phase semihydrogenation of phenylacetylene

Patcharaporn Weerachawanasak [a], Okorn Mekasuwandumrong [b], Masahiko Arai [c], Shin-Ichiro Fujita [c], Piyasan Praserthdam [a], Joongjai Panpranot [a,*]

[a] Center of Excellence on Catalysis and Catalytic Reaction Engineering, Department of Chemical Engineering, Faculty of Engineering, Chulalongkorn University, Bangkok 10330, Thailand
[b] Department of Chemical Engineering, Faculty of Engineering and Industrial Technology, Silpakorn University, Nakhonpathom 73000, Thailand
[c] Division of Chemical Process Engineering, Graduate School of Engineering, Hokkaido University, Sapporo, Japan

ARTICLE INFO

Article history:
Received 15 October 2008
Revised 28 November 2008
Accepted 16 December 2008
Available online 22 January 2009

Keywords:
Pd/TiO_2
Solvothermal synthesis
Liquid-phase semihydrogenation
Phenylacetylene
Strong metal–support interaction
TiO_2 crystallite size

ABSTRACT

Liquid-phase semihydrogenation of phenylacetylene under mild conditions has been investigated on a series of solvothermal-derived nano-TiO_2 supported Pd catalysts with various TiO_2 crystallite sizes in the range of 9–23 nm. As revealed by CO chemisorption and transmission electron microscopy, all the catalysts exhibited strong metal–support interaction (SMSI) when reduced at 500 °C. The catalysts with SMSI show remarkably high catalytic performance in terms of both hydrogenation activities (turnover frequencies (TOFs) 9.1–21.4 s^{-1}) and moderate-high selectivities to styrene (86–90%) at complete conversion of phenylacetylene. Without SMSI effect (the catalysts reduced at 40 °C), styrene selectivity and catalytic activity depended largely on the Pd particle size in which small Pd particles (formed on small crystallite size TiO_2 supports) exhibited lower phenylacetylene conversion and poor styrene selectivity. Moreover, the TOF values of the non-SMSI catalysts were similar to those reported in the literature for other supported Pd catalysts in liquid-phase semihydrogenation of phenylacetylene under mild conditions (TOFs 1.3–2.8 s^{-1}).

1. Introduction

Phenylacetylene removal by selective hydrogenation is a process of great industrial importance because phenylacetylene is a poisoning impurity in styrene feedstocks that causes deactivation of the styrene polymerization catalyst and degrades polystyrene properties [1]. From academic points of view, semihydrogenation of phenylacetylene has often been employed as a model reaction for evaluation of selective hydrogenation catalysts under very mild conditions. New heterogeneous catalysts for the liquid-phase semihydrogenation of phenylacetylene with high styrene selectivity have been continuously developed and reported. Most recent studies focus on preparation of Pd nanoparticles in the forms of dispersed colloids [2] and supported systems [3,4]. The latter, however, may be more commercially attractive for industrial applications due to their better handling properties and low separation problems. In the past, different inorganic and organic materials have been studied as Pd catalyst supports in liquid-phase semihydrogenation of phenylacetylene including carbon [2,5–7], SiO_2 [8,9], γ-Al_2O_3 [10], pumice [11,12], zeolites [4], polymers [1,13], organic matrices [14], pillared clays [15,16], mesostructured silica such as MCM-41, HMS, MSU-X [4,17,18], and TiO_2 [19].

Despite a number of studies on support effects on the reactivity of Pd in such a reaction, controversy regarding structure sensitivity of the reaction still exists. Typically, the turnover frequencies (TOFs) were determined based on the number of palladium sites measured by irreversible CO or H_2 chemisorption. Comparing the results obtained under mild reaction conditions (ambient temperature and low H_2 pressure), the TOF values of Pd catalysts in most of the aforementioned references fall into the same range (about 1–3 s^{-1}) suggesting structure insensitive characteristic of the reaction. Nevertheless, significant increase of the TOFs of Pd nanoparticles by at least fourfold to an order of magnitude has recently been reported on some specially prepared supported Pd catalysts [4,17]. In those studies, the hydrogenation of phenylacetylene was suggested to be structure-sensitive because the TOFs were found to increase with increasing Pd nanoparticle diameter. However, it is noticed that the remarkable high activities of supported Pd catalysts coincidently reported by the two different groups were obtained when Pd nanoparticles were supported on MCM-41 via simultaneous synthesis (simultaneous self-assembling of the MCM-41 and Pd incorporation). Conventional impregnation of palladium on MCM-41 gave similar activities compared to the others [4,18]. We speculate that by simultaneous synthesis, the Pd nanoparticles

* Corresponding author. Fax: +66 2218 6877.
E-mail address: joongjai.p@eng.chula.ac.th (J. Panpranot).

0021-9517/$ – see front matter
doi:10.1016/j.jcat.2008.12.011

may be surrounded by support matrices resulting in the inhibition of CO chemisorption and as a consequence high TOF values being calculated. Such phenomenon was probably similar to the decoration of metal surface by partially reducible metal oxides after high temperature reduction or so-called "the strong metal–support interaction" (SMSI) effect [20].

Thus, it was of interest in this study to verify the effect of SMSI on the catalytic activities and selectivities of Pd catalysts in the liquid phase semihydrogenation of phenylacetylene to styrene. Nanocrystalline TiO_2 powders with various crystallite sizes in the range of 9 to 23 nm were synthesized via solvothermal method and employed as supports for Pd catalysts. It is well-known that TiO_2 manifests SMSI with group VIII transition metals (e.g. Pd, Pt, Ni, and Ir) after high temperature reduction. Significant improvement of catalyst performance due to the SMSI effect has been reported in many catalytic reactions such as CO oxidation [21], methanol synthesis [22], selective acetylene hydrogenation [23–25], and liquid-phase hydrogenation [19,26–33]. Moreover, the degree of SMSI effect on Pd/TiO_2 has been shown to depend largely on both the TiO_2 crystal structure (anatase and rutile) [25–27] and TiO_2 crystallite size [19]. The reduction by H_2 at 200 °C resulted in SMSI for anatase titania supported palladium catalyst, but not for the rutile sample [27]. A very recent study from our group shows the absence of SMSI effect on Pd/TiO_2 when the crystallite size of TiO_2 was fairly large ($\geqslant$0.1 μm) [19]. Therefore, in order to ensure the occurrence of SMSI, the TiO_2 supports used in this study were pure anatase TiO_2 with average crystallite sizes in the nanometer range. The Pd/TiO_2 catalysts were characterized by X-ray diffraction (XRD), N_2 physisorption, scanning electron microscopy (SEM), transmission electron microscopy (TEM), and pulse CO chemisorption. Furthermore, the catalytic properties of the Pd/TiO_2 catalysts were evaluated in the liquid-phase semihydrogenation of phenylacetylene to styrene under mild conditions.

2. Experimental

2.1. Preparation of TiO_2 and Pd/TiO_2 catalysts

The solvothermal-derived nano-TiO_2 was prepared according to the method described in [34] using 15–25 g of titanium(IV) *n*-butoxide (TNB) 97% from Aldrich. The starting material was suspended in 100 ml of 1,4-butanediol in a test tube and then set up in an autoclave. In the gap between the test tube and autoclave wall, 30 ml of solvent was added. After the autoclave was completely purged with nitrogen, it was heated to the desired temperature (300–340 °C) at a rate of 2.5 °C min^{-1} and held at that temperature for 0.5–12 h. Autogenous pressure during the reaction gradually increased as the temperature was raised. After the reaction, the autoclave was cooled to room temperature. The resulting powders were collected by centrifugation after repeated washing with methanol. They were then air-dried at room temperature.

The 1%Pd/TiO_2 catalysts were prepared by the incipient wetness impregnation technique using an aqueous solution of the desired amount of $Pd(NO_3)_2{\cdot}6H_2O$ (Aldrich). The catalysts were dried overnight at 110 °C and then calcined in air at 450 °C for 3 h.

2.2. Catalyst characterization

The specific surface areas, pore volumes, and average pore diameters were determined by N_2 physisorption using a Micromeritics ASAP 2020 automated system and the Brunauer–Emmet–Teller (BET) method. Each sample was degassed under vacuum at <10 μm Hg in the Micromeritics system at 150 °C for 4 h prior to N_2 physisorption. The average pore size was calculated using the BJH desorption method. The XRD patterns of the catalysts were measured from 10° to 80° 2θ using a SIEMENS D5000 X-ray diffractometer and CuK_α radiation with a Ni filter. The catalyst morphology was obtained using a JEOL JSM-35CF scanning electron microscope (SEM) operated at 20 kV. Metal crystallite sizes were obtained using the JEOL JEM 2010 transmission electron microscope that employed a LaB_6 electron gun in the voltage range of 80–200 kV with an optical point to point resolution of 0.23 nm. The amounts of CO chemisorbed on the catalysts were measured using a Micromeritics Chemisorb 2750 automated system with ChemiSoft TPx software. Prior to chemisorption, the sample was reduced in a H_2 flow at the desired temperature for 2 h and then cooled down to ambient temperature in a He flow.

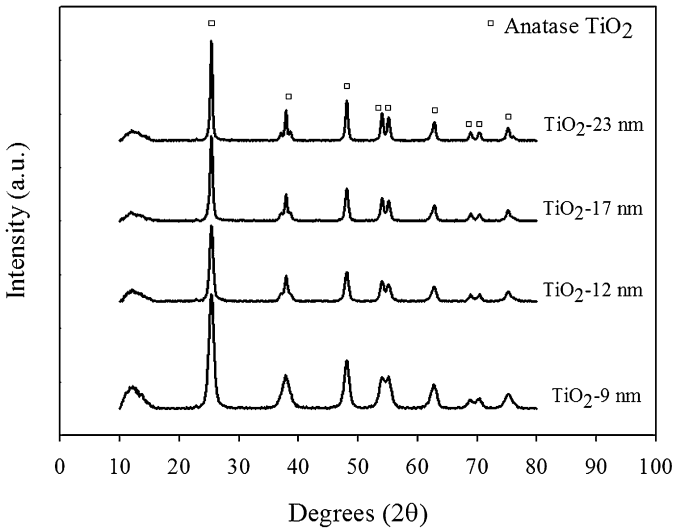

Fig. 1. XRD patterns of the solvothermal-derived TiO_2 with different crystallite sizes.

2.3. Reaction study

Approximately 0.05 g of 1%Pd/TiO_2 catalyst was placed into a 50 ml autoclave. 0.5 ml of phenyl acetylene and 4.5 ml of ethanol (solvent) were mixed in a volumetric flask before being introduced into the autoclave reactor. Afterward the reactor is purged with hydrogen gas. The liquid phase hydrogenation was carried out with H_2 pressure of 1–5 bar and at room temperature for 5–60 min. After the reaction, the vent valve was slowly opened to prevent the loss of product. The product mixture was analyzed by gas chromatography with flame ionization detector (FID) and a GS-alumina capillary column. GC analysis of the reactant after being purged with hydrogen prior to a start of run confirmed that no catalytic reaction occurred before the actual experiment took place.

3. Results and discussion

3.1. Catalyst characterization

In this study, the crystallite size of solvothermal-derived nano-TiO_2 was varied in the range of 9–23 nm by changing the synthesis conditions such as the amount of TNB, reaction temperature, and holding time. Increasing the amount of TNB, reaction temperature, or holding time resulted in an increase of TiO_2 crystallite size. Fig. 1 shows the XRD patterns of the various nano-TiO_2 samples prepared. The characteristic peaks of pure anatase phase titania were observed at $2\theta = 25$, 38, and 48° [35] without contamination of other phases such as rutile and brookite. The average crystallite sizes of TiO_2 were calculated from the full width at half maximum of the XRD peak at $2\theta = 25°$ using the Scherrer equation. The synthesis conditions and the average crystallite size, BET surface

Table 1
Synthesis conditions and physical properties of the nanocrystalline TiO_2.

Sample	TNB (g)	Temp. (°C)	Holding time[a] (h)	XRD crystallite size (nm)			BET surface area[c] (S_1) (m^2/g)	Pore volume[c] (cm^3/g)	Avg. pore diameter[c] (nm)
				As-syn	Reduced[b] at 40 °C	Reduced[b] at 500 °C			
TiO_2-9 nm	15	300	0.5	9	9	11	145	0.42	8.1
TiO_2-12 nm	25	300	2	12	12	13	88	0.37	12.5
TiO_2-17 nm	25	320	6	17	17	18	65	0.38	17.9
TiO_2-23 nm	25	340	12	23	23	23	51	0.32	20.2

[a] Holding time during the solvothermal synthesis of TiO_2 (after the autoclave was heated to 320 °C at a rate of 2.5 °C min^{-1}).
[b] After Pd was impregnated and calcined.
[c] As-syn TiO_2 samples.

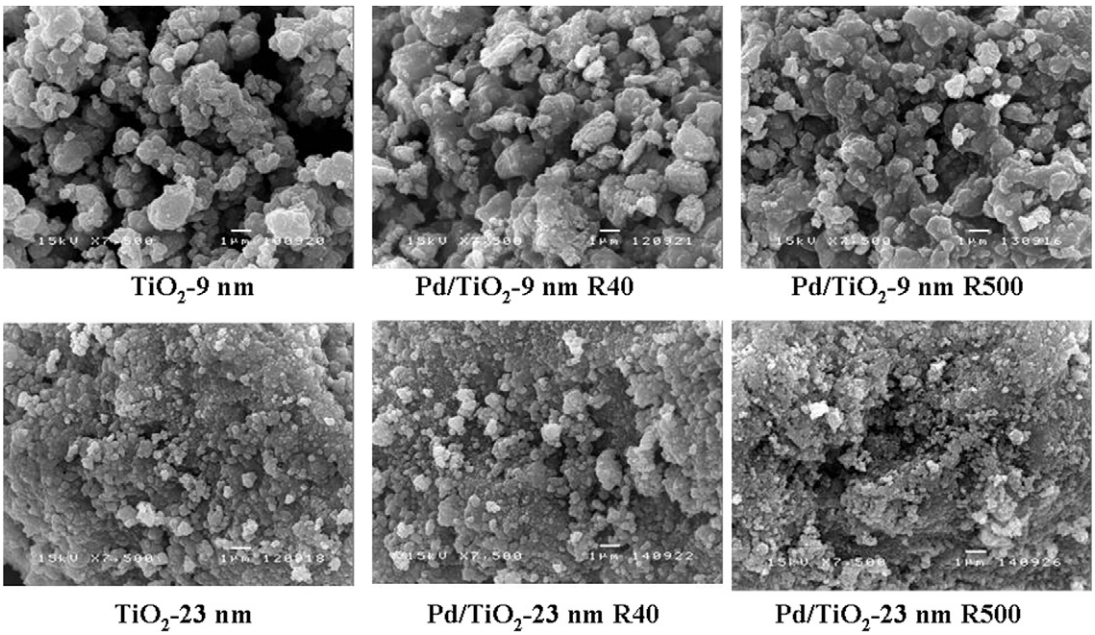

Fig. 2. SEM micrographs of calcined and reduced Pd/TiO_2 catalysts. Reduction temperature = 40 °C (R40), 500 °C (R500).

area, pore volume, and average pore diameter of the obtained TiO_2 samples are given in Table 1. As the average TiO_2 crystallite size increased from 9 to 23 nm, the BET surface area decreased monotonically from 145 to 51 m^2/g. The pore size distribution of various crystallite sizes of TiO_2 supports indicated that the pores of all TiO_2 samples were mesopores (results not shown). After impregnated with approximately 1 wt% Pd, calcined, and reduced at 40 or 500 °C, the crystallite sizes of all the TiO_2 samples as determined by XRD were essentially unaltered except that of the smallest crystallite size TiO_2 (TiO_2-9 nm) in which a slight increase of the TiO_2 crystallite size from 9 to 11 nm was observed. It is generally found that the crystals of small crystallite size show less thermal stability than the crystals of large crystallite size [36].

Fig. 2 shows the SEM micrographs of TiO_2-9 nm and TiO_2-23 nm supports and the corresponding 1 wt% Pd/TiO_2 catalysts after reduced at 40 and 500 °C. The nano-TiO_2 was consisted of irregular shape of very fine particles agglomerated. Morphologies of the reduced 1%Pd/TiO_2 catalysts were not significantly different from the corresponding TiO_2 supports. The particle size and shape of the catalyst particles were also not affected by impregnation of palladium (no changes in the particle size/shape). TEM analysis has been carried out in order to physically measure the TiO_2 crystallite size as well as Pd particle/cluster sizes on the various Pd/TiO_2 catalysts. The TEM results are shown in Fig. 3. The crystallite sizes of the TiO_2 supports were consistent to those obtained from XRD results. The presence of small palladium particles/clusters with an average particle size around 5–6 nm were apparent only on the Pd/TiO_2-23 nm.

The BET surface area, pore volume, average pore diameter, and CO chemisorption results of the various Pd/TiO_2 catalysts are shown in Table 2. The decreases in BET surface areas and pore volumes of the Pd/TiO_2 catalysts compared to the TiO_2 supports suggested that palladium was deposited in some of the pores of the TiO_2. From the CO chemisorption results, it can be seen that for the Pd/TiO_2 catalysts reduced at 40 °C, the amount of CO chemisorption decreased from 18.1×10^{18} to 9.73×10^{18} molecule CO/g cat. as the TiO_2 crystallite size increased from 9 to 23 nm. This was probably due to the lower specific surface area of the larger crystallite size TiO_2 supports that resulted in lower Pd dispersion. For the same catalyst, the amount of CO chemisorption was much lower when reduced at 500 °C. The amounts of CO chemisorption were in the range of 0.9 to 1.31×10^{18} molecule CO/g cat. However, the CO chemisorbed on all the R500 catalysts can be totally restored indicating that the palladium particles did not sinter during high temperature reduction at 500 °C and all the catalysts exhibited the SMSI effect. The Pd^0 metal particles calculated from CO chemisorption results for the catalysts reduced at 40 °C were found to be 3.2–5.9 nm depending on the TiO_2 crystallite size. The results were consistent with TEM analyses. For the catalysts reduced at 500 °C, the Pd^0 metal particle sizes were not determined since it would result in an over-estimation of the particle size. Low amounts of CO or H_2 chemisorption and an over-estimation of Pd particle size have occasionally been reported in other supported

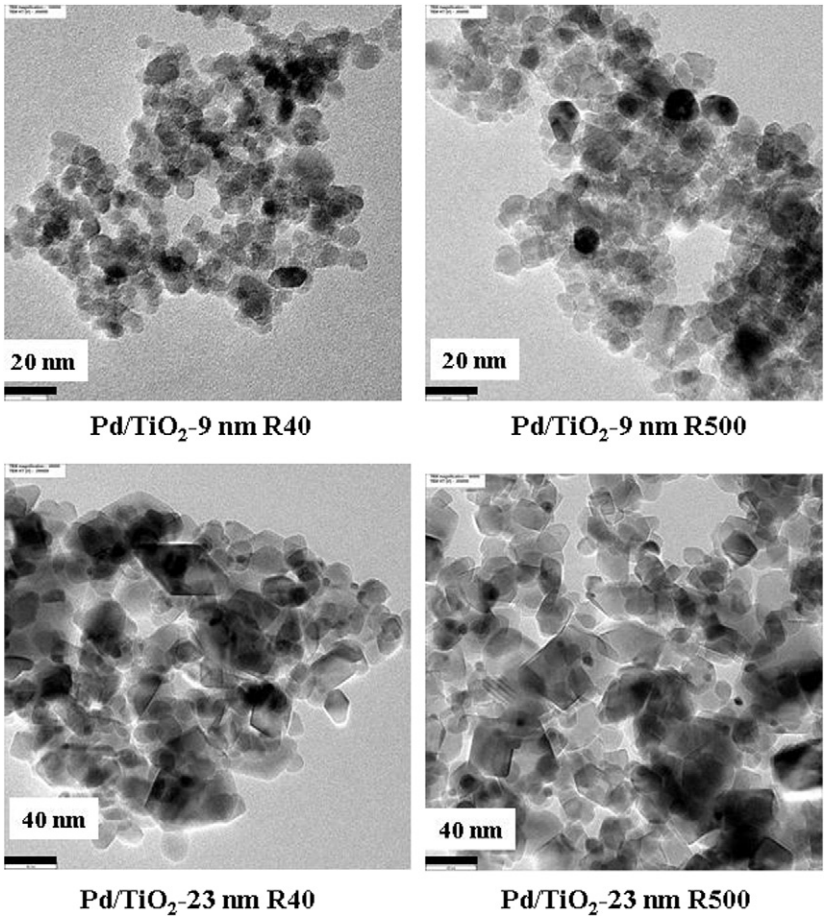

Fig. 3. TEM micrographs of Pd/TiO_2-9 nm and Pd/TiO_2-23 nm reduced at 40 °C (R40) and 500 °C (R500).

Table 2
N_2 physisorption and CO chemisorption results of the Pd/TiO_2 catalysts.

Catalyst	BET surface area (m^2/g)	Pore volume (cm^3/g)	Avg. pore diameter (nm)	CO chemisorption[a] ($\times 10^{-18}$ molecule CO/g cat.)	%Pd dispersion	d_P[d] Pd^0 (nm)
Pd/TiO_2-9 nm R40	135	0.30	6.3	18.1	35.5	3.2
Pd/TiO_2-9 nm R500	89	0.20	6.2	1.31 (18.4)[b]	n.d.[c]	n.d.
Pd/TiO_2-12 nm R40	84	0.31	11.1	15.6	30.5	3.7
Pd/TiO_2-12 nm R500	75	0.30	10.7	1.02 (16.1)	n.d.	n.d.
Pd/TiO_2-17 nm R40	62	0.30	14.3	12.1	23.8	4.7
Pd/TiO_2-17 nm R500	60	0.30	14.2	0.9 (12.0)	n.d.	n.d.
Pd/TiO_2-23 nm R40	47	0.28	19.8	9.73	19.1	5.9
Pd/TiO_2-23 nm R500	42	0.29	19.7	1.11 (11.8)	n.d.	n.d.

[a] Experimental error as determined directly from the measurements = ±5%.
[b] The number in parenthesis indicated the amount of CO chemisorption after the R500 catalyst was re-calcined and re-reduced at 40 °C.
[c] n.d. = not determined.
[d] Based on $d = (1.12/D)$ nm [47], where D = fractional metal dispersion.

Pd catalyst systems such as Pd/MCM-41 prepared via simultaneous synthesis [4,17] and Pd/SiO_2 prepared by one-step flame spray pyrolysis [37]. In those studies, the synthesis of support phase occurred simultaneously with the formation of Pd nanoparticles so the Pd particles may be surrounded by support matrix (i.e., in the form of Si–O group). This could result in the inhibition of CO chemisorption. Such phenomena were somewhat similar to the SMSI effect on Pd/TiO_2. It is generally known that SMSI occurs after reduction at high temperature due to the decoration of the metal surface by partially reducible metal oxides [38,39] and/or by an electron transfer between the support and the metals [40,41] resulting in CO and H_2 chemisorption suppression.

3.2. Catalytic tests

The performance of Pd/TiO_2 catalysts was evaluated in the liquid-phase semihydrogenation of phenylacetylene to styrene in a batch-type stainless steel reactor under mild reaction conditions (H_2 pressure 5 bar and 30 °C). Fig. 4 shows the change in product distribution with reaction time from 5–60 min. In all cases, phenylacetylene was hydrogenated up to nearly 100% conversion within 20 min under the reaction conditions used. The hydrogenation of styrene to ethylbenzene occurred when the concentration of phenylacetylene was sufficiently low indicating a slower parallel reaction pathway for the direct hydrogenation of pheny-

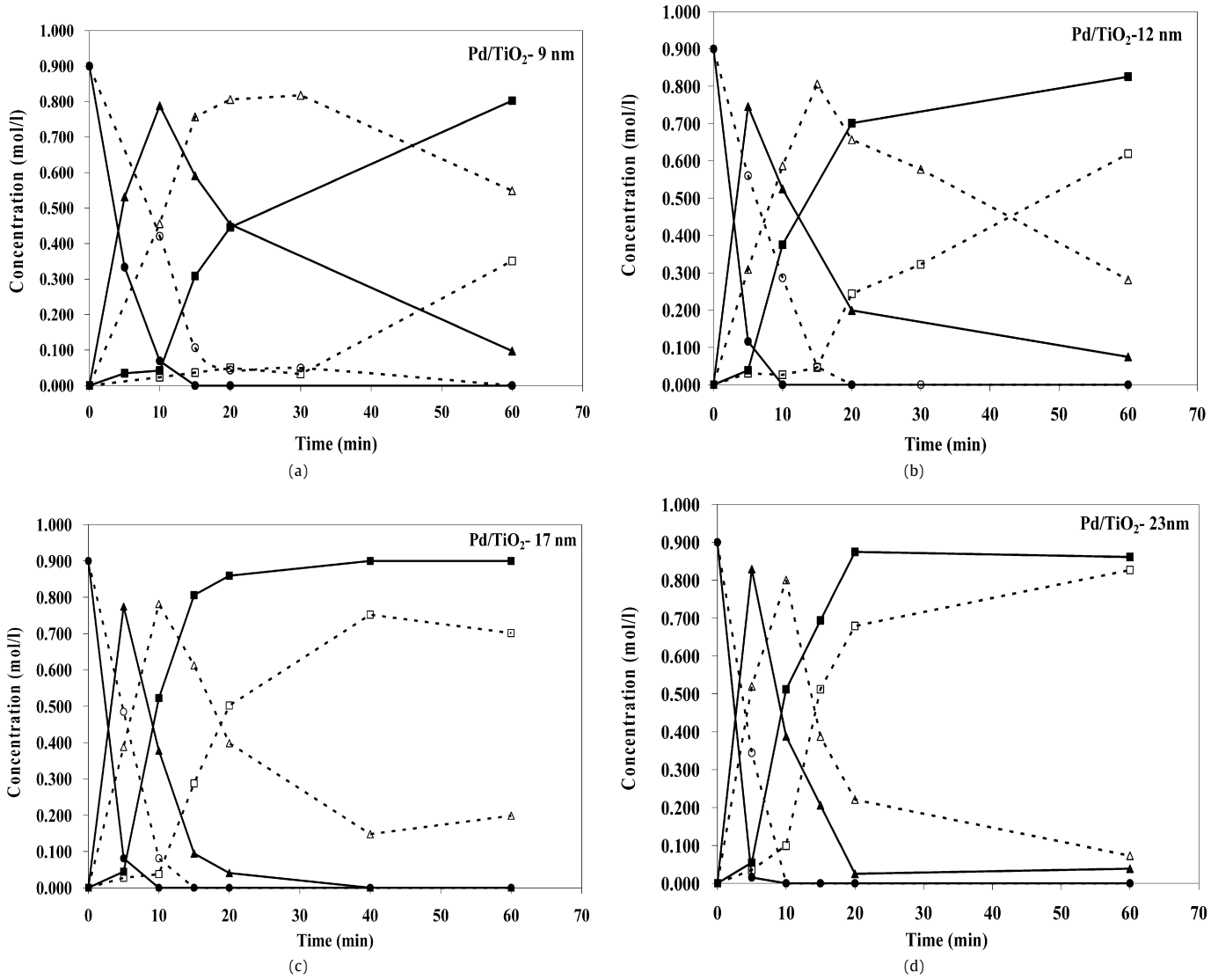

Fig. 4. Liquid-phase semihydrogenation of phenylacetylene over the Pd/TiO_2 catalysts: ○ = phenylacetylene △ = styrene □ = ethylbenzene, solid symbols = Pd/TiO_2 catalysts reduced at 40 °C and open symbols = Pd/TiO_2 catalysts reduced at 500 °C (a) Pd/TiO_2-9 nm, (b) Pd/TiO_2-12 nm, (c) Pd/TiO_2-17 nm, (d) Pd/TiO_2-23 nm (reaction conditions were H_2 pressure = 5 bar and 30 °C).

lacetylene to ethylbenzene. Similar profiles were found for other Pd catalyst systems reported in the literature such as Pd/SiO_2, Pd/C, and commercial Lindlar catalyst in semihydrogenation reaction of alkynes to alkenes [6,42]. The catalyst performance plots (styrene selectivity versus conversion of phenylacetylene) for the various Pd/TiO_2 catalysts are shown in Fig. 5. As can be observed, the catalyst performance was significantly improved when reduced at 500 °C. High styrene selectivity (around 86–90%) was achieved at complete conversion of phenylacetylene for all the catalysts reduced at 500 °C while for the non-SMSI catalysts, the selectivity for styrene significantly dropped to 20–60% when conversion of phenylacetylene reached 100%. Such results confirm the beneficial effect of SMSI in Pd/TiO_2 catalysts on the catalyst performance [8,19]. Charge transfer from the TiO_2 support to Pd during high temperature reduction caused electron enrichment of Pd particles which favored rapid desorption of styrene molecules. Similar results have also been observed for the Pd catalysts supported on organic matrices such as *oligo-p-phenylenterephthalamide* (OPTA) which induces electron transfer from support to metal surface [14]. In gas-phase selective hydrogenation of acetylene to ethylene on Pd/TiO_2 catalysts, the charge transfer from Ti species to Pd weakened the adsorption strength of ethylene on the Pd surface and,

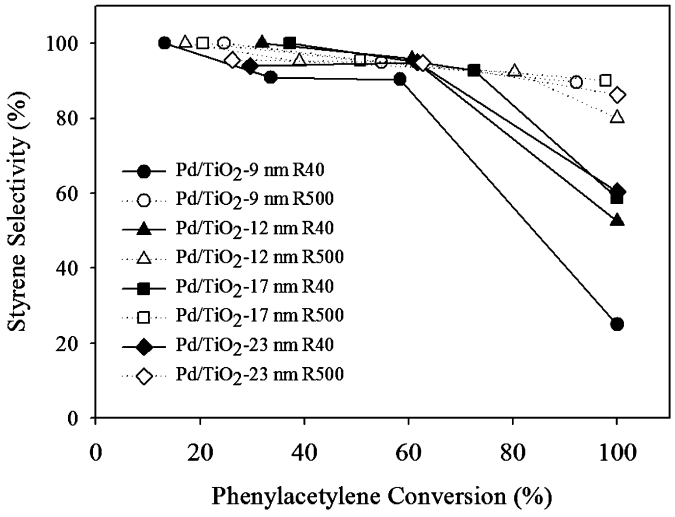

Fig. 5. Performance curves of the various Pd/TiO_2 for selective hydrogenation of phenylacetylene.

Table 3
Catalytic activity of the Pd/TiO_2 catalysts in liquid-phase semihydrogenation of phenylacetylene.

Catalyst	Initial rate[a] (mole products/g cat. s)	TOF[b] (s^{-1})	TOF_{R40}/TOF_{R500}
Pd/TiO_2-9 nm R40	0.14	1.3	
Pd/TiO_2-9 nm R500	0.07	9.1	7.2
Pd/TiO_2-12 nm R40	0.18	1.9	
Pd/TiO_2-12 nm R500	0.09	15.2	8.1
Pd/TiO_2-17 nm R40	0.20	2.8	
Pd/TiO_2-17 nm R500	0.11	20.3	7.3
Pd/TiO_2-23 nm R40	0.16	2.8	
Pd/TiO_2-23 nm R500	0.14	21.4	7.6

[a] Reaction conditions were H_2 pressure = 1 bar, $T = 30\,^{\circ}C$, and reaction time = 10 min.
[b] Based on CO chemisorption results.

hence, higher ethylene selectivity was obtained [23–25]. However, among the R40 series catalysts, the Pd/TiO_2-9 nm R40 exhibited the lowest styrene selectivity at complete conversion of phenylacetylene despite its highest Pd dispersion. This could probably be attributed to longer residence time of styrene on small metal particles [10]. Low dispersed palladium catalysts also showed to be more selective to partial hydrogenation than highly dispersed ones [43].

The initial rates of phenylacetylene hydrogenation and the corresponding TOF values for the eight catalyst samples are given in Table 3. The measured TOF values were based on the experimental results obtained under the reaction conditions that yielded phenylacetylene conversion less than 50% for all the catalysts (H_2 pressure 1 bar 30 °C and reaction time 10 min). For the R40 series (non-SMSI catalysts), the TOFs were not significantly different ranging from 1.3 to 2.8 s^{-1}. The values were very close to those reported in the literature for supported Pd catalysts in liquid-phase hydrogenation of phenylacetylene under mild conditions as summarized in Table 4. The relatively low activity of Pd/TiO_2-9 nm R40 can be attributed to the very small Pd particles being formed on the small crystallite size TiO_2 support. There has been an establishing trend in the literature that specific activity (turnover frequencies) of Pd in selective hydrogenation decreases as Pd particle size decreases especially when the average Pd particle size is very small ($\leqslant$3–5 nm) [4,8,44]. Diminishing activity of small metal particles was probably due to the different band structure characteristics of nano-sized metal compared to bulk metals and that they appear to be electron deficient [45].

For the R500 series, (SMSI catalysts), all the catalysts exhibited very high TOFs (9.1–21.4 s^{-1}). The catalyst performance was proved in terms of both hydrogenation activity and selectivity to styrene. It may be assumed that the presence of SMSI effect favors the formation of active Pd species participating in the reaction. The strong interaction between metal and support and the formation of interfacial Pd–TiO_x sites have also been found in the Pd/TiO_2 catalysts prepared by sol–gel method [28]. They were suggested to be the reasons for the catalysts exhibiting high conversion and high yield towards butyric acid in liquid-phase hydrogenation of maleic anhydride. Remarkable high activities in the hydrogenation of alkynes were also reported for the Pd/MCM-41 catalysts prepared via simultaneous synthesis [4,17] and Pd/SiO_2 prepared by one-step flame spray pyrolysis [37]. It was suggested that simultaneous formation of Pd nanoparticles in the support matrices resulted in the formation of active ensembles for the reaction. In the present study, largest improvement on the catalytic performance for Pd/TiO_2 catalysts reduced at 500 °C was observed on the smallest crystallite size TiO_2 (Pd/TiO_2-9 nm) probably because the formation of substoichiometric TiO_x species was more facile over small crystallite size TiO_2 [46]. The ratios of TOF values of the SMSI and non-SMSI catalysts for the Pd/TiO_2 with different TiO_2 crystallite sizes (see Table 3), however, were quite similar, implying that the degree of SMSI effect on the hydrogenation rate did not depend on the Pd particle size.

4. Conclusions

The presence of SMSI on Pd/TiO_2 catalysts when reduced at 500 °C has proven to produce great beneficial effect on both catalytic hydrogenation activities and selectivities to styrene in liquid-phase semihydrogenation of phenylacetylene under mild conditions (ambient temperature and low H_2 pressure). Without SMSI effect, the turnover frequencies of Pd/TiO_2 were similar to those of other supported Pd catalysts reported in the literature and the catalyst performance depended largely on Pd particle size. In the range of Pd particle size studied (3.2–5.9 nm), the TOF values and styrene selectivity at complete conversion of phenylacetylene increased with increasing Pd particle size.

Acknowledgments

Financial supports from the Thailand Research Fund (TRF) contract RMU50-80030 for Joongjai Panpranot, and the Commission on Higher Education, Thailand are gratefully acknowledged.

Table 4
Comparison of the catalytic activities of supported Pd catalysts in liquid-phase semihydrogenation of phenylacetylene under mild conditions.

Catalyst	BET surface area (m^2/g)	Reactant: Pd molar ratio	Reaction conditions[a]	Pd^0 particle size (nm)	TOFs (s^{-1})	Source
Pd/TiO_2 reduced 40 °C	42–135	1000	$T = 298$ K, $P = 1$ bar	3.2–5.9	1.3–2.8	This work
Pd/TiO_2 reduced 500 °C					9.1–21.4	
Pd/C	136–1343	n/a[b]	$T = 323$ K, $P = 1$ bar	2.5–5.6	0.81–0.96	[3]
Pd/MCM-41	875–970	7300	$T = 323$ K, $P = 1$ bar	2.5–6.8	1.0–4.0	[4]
Pd/Al-MCM-41	928–1066			2.4–7.6	1.0–6.5	
Pd/Al_2O_3	54			2.1	1.0	
Pd/beta zeolite	390			2.4	1.0	
Pd/SiO_2	234–248	1000	$T = 303$ K, $P = 1$ bar	10–12	1.2–1.6	[8]
Pd/pumice	5	1000	$T = 298$ K, $P = 1$ bar	6.3–11.0	6.0–7.7	[11,12]
Pd/organic matrices	n/a	n/a	$T = 283$ K	2.0–12.8	1.3–2.7	[14]
Pd/Al_2O_3, Pd/C	n/a	2500	$T = 298$ K, $P = 1$ bar	1.9, 5.2	0.9, 2.2	[15]
Pd/MCM-41	806–1099	2000	$T = 298$ K, $P = 1$ bar	10–23	5.1–12.9	[17]
Pd/mesostructured silica	910–1469	2500	$T = 298$ K, $P = 1$ bar	0.7–3.2	2.0–4.0	[18]

[a] T = reaction temperature, $P = H_2$ pressure.
[b] n/a = not available.

References

[1] B.R. Maurer, M. Galobardes, US Patent 4,822,936, 1989.
[2] S. Dominguez-Dominguez, A. Berenguer-Murcia, D. Cazorla-Amoros, A. Linares-Solano, J. Catal. 243 (2006) 74.
[3] S. Dominguez-Dominguez, A. Berenguer-Murcia, B.K. Pradhan, D. Cazorla-Amoros, A. Linares-Solano, J. Phys. Chem. C 112 (2008) 3827.
[4] S. Dominguez-Dominguez, A. Berenguer-Murcia, A. Linares-Solano, D. Cazorla-Amoros, J. Catal. 257 (2008) 87.
[5] R.V. Chaudhari, R. Jaganathan, D.S. Kolhe, Ind. Eng. Chem. Prod. Res. Dev. 25 (1986) 375.
[6] S.D. Jackson, L.A. Shaw, Appl. Catal. 134 (1996) 91.
[7] F.M. Bautista, J.M. Campelo, A. Garcia, D. Luna, J. Marinas, R.A. Quiros, A.A. Romero, Catal. Lett. 52 (1998) 205.
[8] J. Panpranot, K. Phandinthong, T. Sirikajorn, M. Arai, P. Praserthdam, J. Mol. Catal. 261 (2007) 29.
[9] S.S. Mahmoud, I.M. Arafa, O.I. Sheikha, Asian J. Chem. 12 (2000) 1047.
[10] C. Del Angel, J.L. Benitez, React. Kinet. Catal. Lett. 51 (1993) 547.
[11] L. Guczi, Z. Schay, Gy. Stefler, L.F. Liotta, G. Deganello, A.M. Venezia, J. Catal. 182 (1999) 456.
[12] D. Duca, L.F. Liotta, G. Deganello, J. Catal. 154 (1995) 69.
[13] M. Terasawa, H. Yamamoto, K. Kaneda, T. Imanaka, S. Teranishi, J. Catal. 57 (1979) 315.
[14] F. Arena, G. Cum, R. Gallo, A. Parmaliana, J. Mol. Catal. A 110 (1996) 235.
[15] A. Mastalir, Z. Király, J. Catal. 220 (2003) 372.
[16] A. Mastalir, Z. Király, F. Berger, Appl. Catal. A 269 (2004) 161.
[17] A. Papp, A. Molnar, A. Mastalir, Appl. Catal. A 289 (2005) 256.
[18] N. Marin-Astorga, G. Pecchi, T.J. Pinnavaia, G. Alvez-Manoli, P. Reyes, J. Mol. Catal. A 247 (2006) 145.
[19] P. Weerachawanasak, P. Praserthdam, M. Arai, J. Panpranot, J. Mol. Catal. A 279 (2007) 133.
[20] S.J. Tauster, S.C. Fung, R.L. Garten, J. Am. Chem. Soc. 100 (1978) 170.
[21] H. Zhu, Z. Qin, W. Shan, W. Shen, J. Wang, J. Catal. 233 (2005) 41.
[22] N. Tsubaki, K. Fujimoto, Top. Catal. 22 (2003) 325.
[23] H.K. Jung, W.S. Eun, J.K. Woo, D.P. Jae, H.M. Sang, J. Catal. 208 (2002) 310.
[24] J. Panpranot, K. Kontapakdee, P. Praserthdam, J. Phys. Chem. B 110 (2006) 8019.
[25] J. Panpranot, K. Kontapakdee, P. Praserthdam, Appl. Catal. A 314 (2006) 128.
[26] Y. Li, B. Xu, Y. Fan, N. Feng, A. Qiu, J. Miao, J. He, H. Yang, Y. Chen, J. Mol. Catal. A 216 (2004) 107.
[27] P.S. Kumbhar, Appl. Catal. A 96 (1993) 241.
[28] J. Xu, K. Sun, L. Zhang, Y. Ren, X. Xu, Catal. Commun. 6 (2005) 462.
[29] P. Reyes, H. Rojas, J.L.G. Fierro, Appl. Catal. A 248 (2003) 59.
[30] U.K. Singh, M.A. Vannice, Stud. Surf. Sci. Catal. 130 (2000) 497.
[31] P. Reyes, H. Rojas, G. Pecchi, J.L.G. Fierro, J. Mol. Catal. A 179 (2002) 293.
[32] U.K. Singh, M.A. Vannice, J. Mol. Catal. A 163 (2000) 233.
[33] J. Xiong, J. Chen, J. Zhang, Catal. Commun. 8 (2007) 345.
[34] W. Payakgul, O. Mekasuwandumrong, V. Pavarajarn, P. Praserthdam, Ceram. Int. 31 (2005) 391.
[35] S.S. Watson, D. Beydoun, J.A. Scott, R. Anal, Chem. Eng. J. 95 (2003) 213.
[36] H. Kominami, M. Kohno, Y. Takada, M. Inoue, T. Inui, Y. Kera, Ind. Eng. Chem. Res. 38 (1999) 3925.
[37] S. Somboonthanakij, O. Mekasuwandumrong, J. Panpranot, T. Nimmanwudtipong, R. Strobel, S.E. Pratsinis, P. Praserthdam, Catal. Lett. 119 (2007) 346.
[38] J. Santos, J. Phillips, J.A. Dumesic, J. Catal. 81 (1983) 147.
[39] G.B. Raupp, J.A. Dumesic, J. Catal. 95 (1985) 587.
[40] J.M. Herrmann, M. Gravelle-Rumeau-Maillot, P.C. Gravelle, J. Catal. 104 (1987) 136.
[41] P. Chou, M.A. Vannice, J. Catal. 104 (1987) 1.
[42] T.A. Nijhuis, G. van Koten, J.A. Moulijn, Appl. Catal. A 238 (2003) 259.
[43] G. del Angel, J.L. Benitez, J. Mol. Catal. A 94 (1994) 409.
[44] N. Semagina, A. Renken, L. Kiwi-Minsker, J. Phys. Chem. C 111 (2007) 13933.
[45] A. Molnar, A. Sarkany, M. Varga, J. Mol. Catal. 173 (2001) 185.
[46] P. Panagiotopoulou, A. Christodoulakis, D.I. Kondarides, S. Boghosian, J. Catal. 240 (2006) 114.
[47] N. Mahata, V. Vishwanathan, J. Catal. 196 (2000) 262.